

# Parameter Estimation Method for Dual-Stator Permanent Magnet Synchronous Motor Based on Incremental Inductance

Cheon-Ho Song<sup>1</sup>, Ji-Hyeon Lee<sup>1</sup>, and Myung-Seop Lim<sup>2</sup>

<sup>1</sup>Department of Automotive Engineering (Automotive-Computer Convergence), Hanyang University, Seoul 04763, Republic of Korea

<sup>2</sup>Department of Automotive Engineering, Hanyang University, Seoul 04763, Republic of Korea

The dual inverter and dual stator system is suitable for air mobility due to its redundant system. Motor analysis for transportation should encompass not only electromagnetic characteristics but also drive and multiphysics systems to account for real operating conditions. To reduce the considerable time of system integrated analysis, especially those involving drive and multiphysics systems, a parameter-based model can be employed as a substitute for the finite element analysis (FEA) co-simulation. Therefore, an accurate and fast parameter-deriving method is required. The conventional method, the frozen-permeability method, is accurate but time-consuming because the dual stator system has doubled inputs. In this article, a parameter estimation method based on the incremental method is proposed to consider a dual stator motor. Subsequently, the frozen-permeability method and the proposed method are compared to assess their accuracy. The results show that the proposed method can acquire accurate data faster than the frozen-permeability method. In addition, experiments are conducted to validate the parameter-deriving methods.

*Index Terms*—Dual stator, frozen-permeability, incremental inductance, parameter-based model.

## I. INTRODUCTION

DUAL stator motor has improved characteristics over other motor types such as high power density and robust fault tolerance [1]. It can be adjusted in a dual inverter system because windings are separated. These characteristics are suitable for air mobility because of its redundant system that can be dealing with fault conditions. Some motors are separated by dual winding in single stators [2], [3] and others are dual winding in dual stators [1], [4].

Analysis of motors for transportation should consider more complex conditions than other applications to ensure safety. There is ongoing research in system-integrated analysis, including motor drive analysis, thermal analysis, and vibration and noise analysis, to address real operating conditions. Co-simulation between motor and drive can consider motor control performance and switching fluctuations [5], [6]. There is the problem of being time consuming because the switching frequency is higher than the frequency of the motor source when using finite element analysis (FEA). In addition, drive cycle analysis for driving efficiency tests should be conducted [7]. Whole vehicle performance is simulated by system-integrated simulation including motor, battery, control unit, and so on [8]. However, a common problem is the long duration of FEA.

A parameter-based model, utilizing a lookup table dataset acquired through pre-simulated FEA, can reduce the time required for determining motor performance. The parameters

include flux-linkage, inductance, and loss data represented as a lookup table. It is utilized to control integrated analysis and multiphysics analysis because of its simple data volume and fast data interaction. It is utilized in some motor research because of its accurate and convenient usage [8], [9], [10]. In addition, the exact estimation of parameters enhances fault tolerance and improves control performance. Therefore, accurate parameter prediction should be a prerequisite for system-integrated analysis.

Conventional methods of estimating parameters are the frozen-permeability method [11] and incremental inductance [12]. The frozen-permeability method involves utilizing preexisting permeability data in FEA. Each phase winding is excited with the unit current to determine its inductance. This method is accurate and reliable; however, the time required for loading permeability data can be time-consuming. The incremental inductance method involves using small flux changes corresponding to small changes in current. This method is faster than the frozen-permeability method due to the absence of the permeability loading process. In a dual stator system, an additional cross-coupling inductance matrix between each stator should be taken into consideration. This cannot be considered in the conventional incremental inductance method.

In this article, a modified incremental inductance method that considers the mutual inductance between dual stators is proposed. To distinguish between self-inductance (within a single stator) and mutual inductance (between dual stators), an offset flux separated by the ratio of self and mutual flux is suggested. The advantages and features of the proposed method are introduced by comparing it with the frozen-permeability method, along with experimental results. As a result, the proposed method is as accurate as the conventional method and provides a faster process for estimating the

Manuscript received 24 March 2024; accepted 7 June 2024. Date of publication 3 July 2024; date of current version 27 August 2024. Corresponding author: M.-S. Lim (e-mail: myungseop@hanyang.ac.kr).

Color versions of one or more figures in this article are available at <https://doi.org/10.1109/TMAG.2024.3422800>.

Digital Object Identifier 10.1109/TMAG.2024.3422800

0018-9464 © 2024 IEEE. Personal use is permitted, but republication/redistribution requires IEEE permission. See <https://www.ieee.org/publications/rights/index.html> for more information.

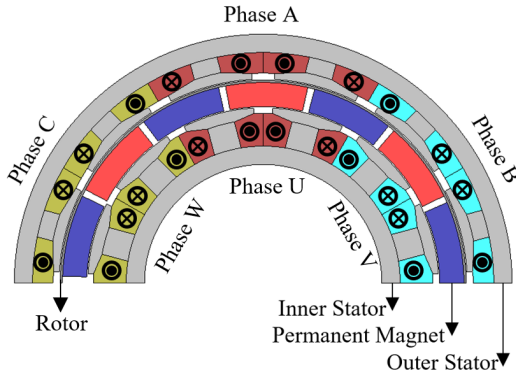


Fig. 1. Mechanical structure of the dual stator PMSM.

parameters of a dual stator permanent magnet synchronous motor (PMSM) for air mobility.

## II. ANALYSIS MODEL

In this chapter, a model of a dual stator PMSM is introduced. In addition, the voltage and torque equations of the motor are presented. The equation of the dual-stator motor is referenced from [1].

The conceptual model is depicted in Fig. 1. The stators are positioned on the inner and outer sides, with each stator having windings that are electrically separated from each other. The rotor, comprised of a retainer and permanent magnets, is positioned between the inner and outer stators.

Due to its dual-stator (winding) structure, this model exhibits a more complex inductance matrix. In this article, the inductance within a single winding is referred to as self-inductance ( $L$ ). Furthermore, the inductance between the inner and outer windings is denoted as mutual inductance ( $M$ ). The details of the inductance matrix are shown below

$$L_{dqz} = \begin{bmatrix} L_{d1d1} & L_{d1q1} & L_{d1z1} & M_{d1d2} & M_{d1q2} & M_{d1z2} \\ L_{q1d1} & L_{q1q1} & L_{q1z1} & M_{q1d2} & M_{q1q2} & M_{q1z2} \\ L_{z1d1} & L_{z1q1} & L_{z1z1} & M_{z1d2} & M_{z1q2} & M_{z1z2} \\ M_{d2d1} & M_{d2q1} & M_{d2z1} & L_{d2d2} & L_{d2q2} & L_{d2z2} \\ M_{q2d1} & M_{q2q1} & M_{q2z1} & L_{q2d2} & L_{q2q2} & L_{q2z2} \\ M_{z2d1} & M_{z2q1} & M_{z2z1} & L_{z2d2} & L_{z2q2} & L_{z2z2} \end{bmatrix}. \quad (1)$$

The subscripts “ $d$ ” and “ $q$ ” refer to the  $d - q$  transformed axis, while “ $z$ ” signifies the zero-sequence component. The zero-sequence component is disregarded when the winding connection is grounded. Therefore, in this article, the zero-sequence component term is not used. In addition, in the subscript notation, the number “1” corresponds to the outer-side winding, while the number “2” corresponds to the inner-side winding

$$\lambda_{dq} = \begin{bmatrix} \lambda_{d1} \\ \lambda_{q1} \\ \lambda_{d2} \\ \lambda_{q2} \end{bmatrix} = L_{dq} \times \begin{bmatrix} i_{d1} \\ i_{q1} \\ i_{d2} \\ i_{q2} \end{bmatrix} + \begin{bmatrix} \Psi_{fd1} \\ \Psi_{fq1} \\ \Psi_{fd2} \\ \Psi_{fq2} \end{bmatrix}. \quad (2)$$

The next step involves flux linkages, determined by the inductance matrix,  $d - q$  transformed currents, and the flux linkages of the permanent magnet. Flux-linkages,  $\lambda$ , of dual stator PMSM are divided into set 1 and set 2. Normally,

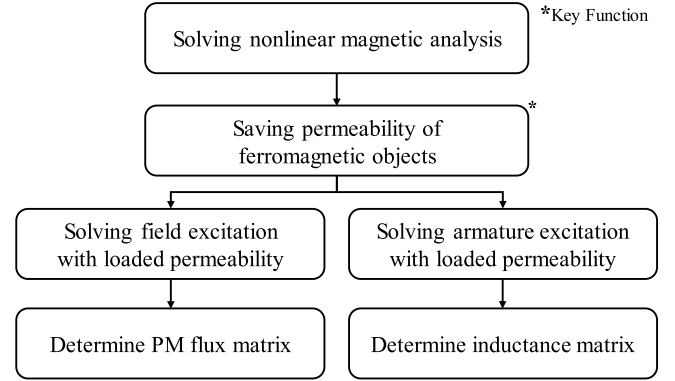


Fig. 2. Flowchart of frozen-permeability method for inductance.

zero-sequence components are ignored because these are not affected by torque generation. In (2),  $L_{dq}$  is identical to (1) without zero-sequence components.  $\Psi_{fdq}$  is the flux-linkage of the field. The flux-linkage matrix consists of the product of inductance and current and the sum of the fluxes by the field

$$V_{o1,2} = \sqrt{V_{od1,2}^2 + V_{oq1,2}^2} = \omega \sqrt{\lambda_{d1,2}^2 + \lambda_{q1,2}^2}. \quad (3)$$

Following that, the output voltage ( $V_o$ ) term without resistance voltage drop is derived from the flux linkages and the rotational speed

$$T = \frac{P_o}{\omega} = \frac{V_{od1}i_{d1} + V_{oq1}i_{q1} + V_{od2}i_{d2} + V_{oq2}i_{q2}}{\omega} = \frac{3}{2} pp(\lambda_{d1}i_{q1} + \lambda_{q1}i_{d1} + \lambda_{d2}i_{q2} + \lambda_{q2}i_{d2}). \quad (4)$$

The torque is determined by dividing the output power ( $P_o$ ), which is the product of voltage and current, by the rotational speed. Here, a  $3/2$  term is required because parameters are determined by magnitude invariance assumption.  $pp$  represents the pole-pair.

## III. METHODS OF DETERMINATION OF INDUCTANCE

In this chapter, methods for determining inductance are introduced. The first method is the conventional frozen-permeability method, and the second method is a proposed incremental inductance method modified to account for the dual stator structure. To explain each method, a flowchart is presented initially, followed by the key mechanism. Finally, analytical torque and FEA torque results are compared to validate the accuracy of the parameters.

### A. Method 1: Frozen-Permeability Method

The frozen-permeability method employs FEA. Its mechanism involves saving the permeability of each element according to the total analysis time steps. PMSM has two excitation sources: one is the winding current, and the other is the permanent magnet source. As a result, frozen-permeability analysis should be conducted twice to account for each excitation source. The detail of this method is shown in Fig. 2 as a flowchart.

Fig. 3 shows the key function mentioned in Fig. 1. Following the non-linear magnetic analysis, the permeabilities of all

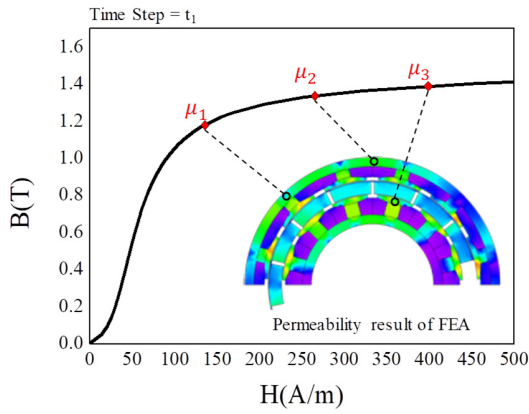


Fig. 3. Key function of frozen-permeability at single time step.

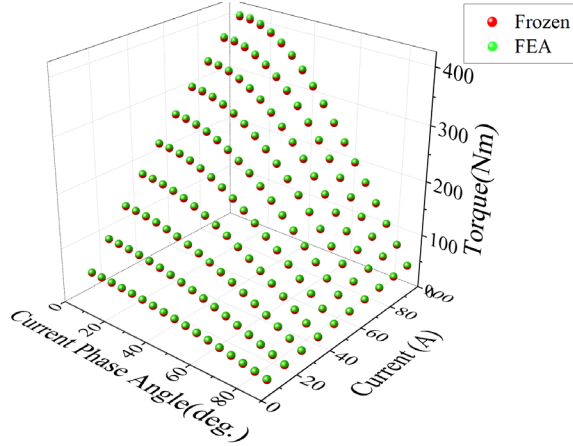


Fig. 4. Torque determined by frozen-permeability method and FEA.

elements are saved. The time required for saving and loading differs based on the number of elements and time steps.

To assess the accuracy of parameters determined by frozen permeability, a torque comparison is conducted. The reference is the torque determined by FEA, while the torque determined by frozen permeability is calculated using (4). Fig. 4 presents the torque comparison, revealing an average error of 0.65%. The torque determined by the frozen permeability method demonstrates accurate results.

### B. Method 2: Proposed Incremental Inductance Method

The conventional incremental method is unable to consider the mutual inductance coupling between the inner and outer windings of dual stators, particularly the  $q$ -axis inductance, due to the absence of offset flux, such as PM flux. Therefore, this article proposes a modified incremental method customized for dual-stator PMSM.

The key mechanism of the incremental inductance method for dual stator PMSM lies in distinguishing between self and mutual components at the  $q$ -axis. In Fig. 5, the flowchart of the proposed method is shown.

The proposed method is more two steps than the conventional incremental method. The initial distinction lies in the incremental current along the  $q$ -axis, utilized to ascertain the incremental inductance (denoted as “inc”) and the offset flux. The second point involves the definition of  $q$ -axis apparent inductance (denoted as “app”), derived from the incremental

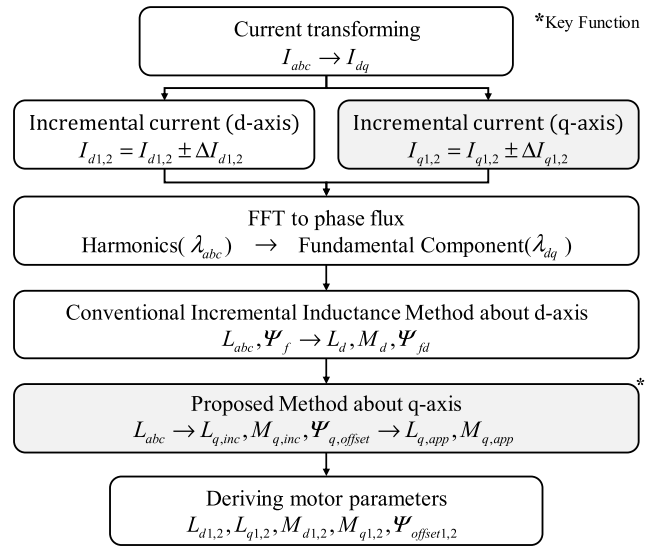


Fig. 5. Flowchart of proposed method.

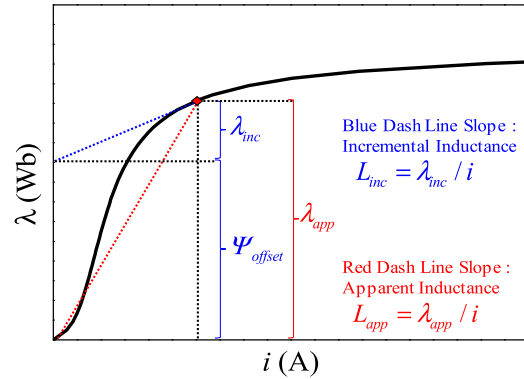


Fig. 6. Description of incremental and apparent inductance.

inductance. The concept of apparent and incremental is well described in [12] and Fig. 6 shows it briefly. The incremental method makes incremental flux-linkage and offset flux. The sum of incremental flux and offset flux is the apparent flux.

The  $q$ -axis inductance should be divided into self and mutual inductance. To achieve this, the offset flux should also be decomposed into self and mutual components. In this article, the self and mutual offset flux are divided using the ratio between self and mutual incremental flux linkages.

The summary and equations of the proposed method are shown in Fig. 7. The upper subscript “prime” means incremental inductance of the  $q$ -axis. The total process is divided into the  $d$ -axis and  $q$ -axis. First, the  $d$ -axis is considered, and the incremental inductance is defined. Subsequently, the offset flux, represented as field flux-linkage, is defined. The  $d$ -axis process concludes at this step with (5)–(7). Second, the  $q$ -axis is considered, and incremental inductance is defined with (8), (9). Then,  $q$ -axis offset flux is defined and, self and mutual components are divided using incremental flux ratio with (10)–(12). Finally, the sum between incremental flux and offset flux makes apparent inductance with (13) and (14).

Derived parameters using the proposed method are validated by comparing the torque with FEA.

Fig. 8 shows the torque results. Whole points show little difference between the torque of the proposed method and

	D-axis	Q-axis
Define Inductance	$L_d = \frac{\lambda_{d+} - \lambda_{d-}}{i_{d+} - i_{d-}}$ (5)	$L'_q = \frac{\lambda_{q+} - \lambda_{q-}}{i_{q+} - i_{q-}}$ (8)
	$M_{d1d2} = \frac{\lambda_{d1+} - \lambda_{d1-}}{i_{d2+} - i_{d2-}}$ (6)	$M'_{q1q2} = \frac{\lambda_{q1+} - \lambda_{q1-}}{i_{q2+} - i_{q2-}}$ (9)
Define Offset Flux	$\Psi_{f1} = \lambda_{d1} - L_{d1}i_{d1} - M_{d1d2}i_{d2}$ (7)	$\Psi_{q\_offset} = \lambda_{q1} - (L'_{q1}i_{q1} + M'_{q1q2}i_{q2})$ (10)
		$\Psi_{q\_offset,L1} = \Psi_{q\_offset} \times \frac{L'_{q1}i_{q1}}{L'_{q1}i_{q1} + M'_{q1}i_{q2}}$ (11)
		$\Psi_{q\_offset,M1} = \Psi_{q\_offset} \times \frac{M'_{q1}i_{q2}}{L'_{q1}i_{q1} + M'_{q1}i_{q2}}$ (12)
Redefine Inductance		$L_{q1} = \frac{L'_{q1}i_{q1} + \Psi_{q\_offset,L1}}{i_{q1}}$ (13)
		$M_{q1} = \frac{M'_{q1}i_{q2} + \Psi_{q\_offset,M1}}{i_{q2}}$ (14)

Fig. 7. Flow and equations of proposed method.

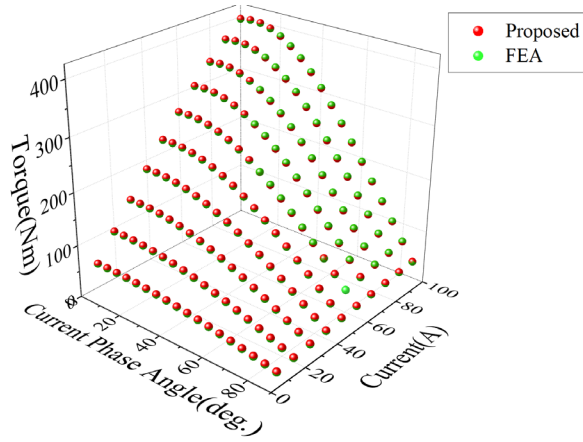


Fig. 8. Torque determined by proposed method and FEA.

FEA. Total average is 0.26%. It means that the whole torques determined by the proposed method are accurate.

### C. Differences Between Frozen-Permeability and Proposed Method

The incremental inductance method ignores the cross-magnetization between the  $d$ -axis and the  $q$ -axis. In contrast, the frozen-permeability method considers the entire inductance matrix. To illustrate this difference, this section presents the inductance matrix.

First, of comparison, the inductance matrix is shown below

$$\lambda_{dq\_frozen} = \begin{bmatrix} L_{d1d1} & L_{d1q1} & M_{d1d2} & M_{d1q2} \\ L_{q1d1} & L_{q1q1} & M_{q1d2} & M_{q1q2} \\ M_{d2d1} & M_{d2q1} & L_{d2d2} & L_{d2q2} \\ M_{q2d1} & M_{q2q1} & L_{q2d2} & L_{q2q2} \end{bmatrix} \begin{bmatrix} i_{d1} \\ i_{q1} \\ i_{d2} \\ i_{q2} \end{bmatrix} + \begin{bmatrix} \Psi_{fd1} \\ \Psi_{fq1} \\ \Psi_{fd2} \\ \Psi_{fq2} \end{bmatrix}. \quad (15)$$

Equation (15) shows the flux matrix using the frozen-permeability method. The whole inductance matrix including

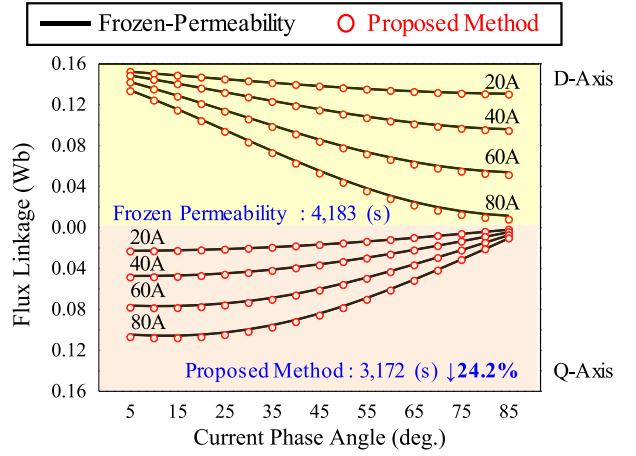


Fig. 9. Flux-linkages determined by frozen-permeability method and proposed method.

TABLE I  
FEATURES COMPARISON BETWEEN FROZEN-PERMEABILITY METHOD AND PROPOSED METHOD

Method	Computing Time	Estimation Accuracy	d-q cross components
Frozen	Slow	Moderate	Considered
Proposed	Fast	Moderate	Ignored

$d-q$  cross-magnetizing components ( $L_{dq}$ ,  $M_{dq}$ ,  $L_{qd}$ ,  $M_{qd}$ ) can be estimated

$$\lambda_{dq\_proposed} = \begin{bmatrix} L_{d1d1} & 0 & M_{d1d2} & 0 \\ 0 & L_{q1q1} & 0 & M_{q1q2} \\ M_{d2d1} & 0 & L_{d2d2} & 0 \\ 0 & M_{q2q1} & 0 & L_{q2q2} \end{bmatrix} \begin{bmatrix} i_{d1} \\ i_{q1} \\ i_{d2} \\ i_{q2} \end{bmatrix} + \begin{bmatrix} \Psi_{fd1} \\ 0 \\ \Psi_{fd2} \\ 0 \end{bmatrix}. \quad (16)$$

Equation (16) shows the flux-linkages matrix of the proposed method. In this inductance matrix,  $d-q$  cross-magnetization components are ignored. The incremental inductance method has the assumption that is field flux-linkages only on the  $d$ -axis. Therefore, field flux-linkages are only  $d$ -axis component.

Although the inductance matrix differs between the two methods, the calculated flux-linkages of the  $d-q$ -axis are identical in both approaches. Fig. 9 shows flux-linkages and consumption of time. The proposed method can reduce analysis time by approximately 24.2%.

In Table I, a summary of the differences between the two methods is shown. The proposed method has a faster computing time. The accuracy of flux-linkage is at the same level as shown in Fig. 9. It is faster than the conventional method but cannot consider  $d-q$  cross-magnetizing components. However, the total flux-linkage estimation is accurate.

## IV. VALIDATION

In this chapter, inductance determination methods are validated with experiment data. A test motor is manufactured to establish a laboratory test environment. This motor is a

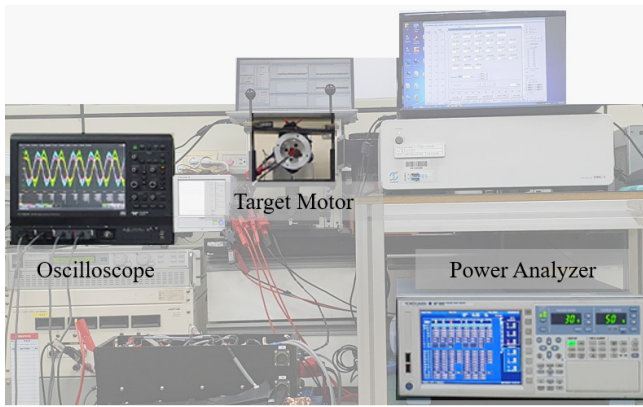


Fig. 10. Experiment set.

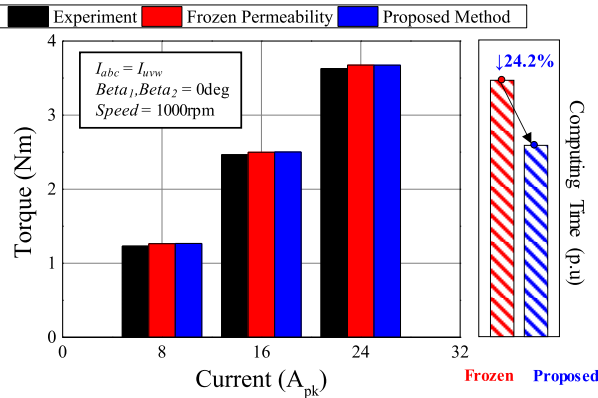


Fig. 11. Comparing the torque according to deriving methods.

reduced-power model with a 2 kW rating, while maintaining the structure of the motor introduced in this article. Fig. 10 shows the setup of the test motor.

Fig. 11 shows a comparison of torque data between the experiment, the frozen-permeability method, and the proposed method. The test conditions are set with identical magnitudes of currents, where the current phase is denoted as beta, and the speed is set at 1000 r/min. The average torque error when using the frozen-permeability method is 1.77%, while it is 1.88% when employing the proposed method. As we did not consider no-load iron losses and friction losses, the results appear reasonable.

This experiment is conducted at a slow speed to avoid errors caused by rotating harmonics, mechanical losses, and iron losses. This condition relatively reduces the error between measurement and estimation.

## V. CONCLUSION

In this article, an incremental inductance method for dual-stator PMSM is proposed. This method overcomes the

limitations of conventional incremental inductance methods that do not consider mutual components between two stator windings. In addition, the computational time is faster compared to the frozen-permeability method. The accuracy of the proposed method is validated through comparisons with the frozen-permeability method and experimental results. By utilizing this method, a parameter-based model can be determined with both accuracy and fast analysis time.

## ACKNOWLEDGMENT

This work was supported by the National Research Foundation of Korea (NRF) funded by Korean Government [Ministry of Science and ICT (MSIT)] under Grant RS-2023-00207865.

## REFERENCES

- [1] S. Hwang, D. Son, S. Park, G. Lee, Y. Yoon, and M. Lim, "Design and analysis of dual stator PMSM with separately controlled dual three-phase winding for eVTOL propulsion," *IEEE Trans. Transport. Electric.*, vol. 8, no. 4, pp. 4255–4264, Dec. 2022.
- [2] Y. Yang, Y. Chen, W. Hao, X. Guo, and Z. Zheng, "A novel dual-redundancy permanent magnet synchronous motor with small teeth," *IEEE Trans. Magn.*, vol. 59, no. 2, pp. 1–10, Feb. 2023.
- [3] J. Huang, Y. Sui, Z. Yin, Z. Yuan, and P. Zheng, "A novel high torque density dual three-phase PMSM with low space harmonic content," *IEEE Trans. Magn.*, vol. 58, no. 8, pp. 1–7, Aug. 2022.
- [4] S. Asgari and M. Mirsalim, "A novel dual-stator radial-flux machine with diametrically magnetized cylindrical permanent magnets," *IEEE Trans. Ind. Electron.*, vol. 66, no. 5, pp. 3605–3614, May 2019.
- [5] K. Ahn, A. E. Bayrak, and P. Y. Papalambros, "Electric vehicle design optimization: Integration of a high-fidelity interior-permanent-magnet motor model," *IEEE Trans. Veh. Technol.*, vol. 64, no. 9, pp. 3870–3877, Sep. 2015.
- [6] W. Zhao, M. Cheng, X. Zhu, W. Hua, and X. Kong, "Analysis of fault-tolerant performance of a doubly salient permanent-magnet motor drive using transient cosimulation method," *IEEE Trans. Ind. Electron.*, vol. 55, no. 4, pp. 1739–1748, Apr. 2008.
- [7] A. Fatemi, D. M. Ionel, M. Popescu, Y. C. Chong, and N. A. O. Demerdash, "Design optimization of a high torque density spoke-type PM motor for a formula E race drive cycle," *IEEE Trans. Ind. Appl.*, vol. 54, no. 5, pp. 4343–4354, Sep./Oct. 2018.
- [8] A. J. P. Ortega, S. Das, R. Islam, and M. B. Kouhshahi, "High-fidelity analysis with multiphysics simulation for performance evaluation of electric motors used in traction applications," *IEEE Trans. Ind. Appl.*, vol. 59, no. 2, pp. 1273–1282, Mar. 2023.
- [9] B. Praslicka, C. Ma, and N. Taran, "A computationally efficient high-fidelity multi-physics design optimization of traction motors for drive cycle loss minimization," *IEEE Trans. Ind. Appl.*, vol. 59, no. 2, pp. 1351–1360, Mar. 2023.
- [10] J.-H. Lee, Y.-C. Kwon, and S.-K. Sul, "High-fidelity induction motor simulation model based on finite element analysis," *IEEE Trans. Ind. Electron.*, vol. 69, no. 10, pp. 9872–9883, Oct. 2022.
- [11] J. A. Walker, D. G. Dorrell, and C. Cossar, "Flux-linkage calculation in permanent-magnet motors using the frozen permeabilities method," *IEEE Trans. Magn.*, vol. 41, no. 10, pp. 3946–3948, Oct. 2005.
- [12] T. W. Nehl, F. A. Fouad, and N. A. Demerdash, "Determination of saturated values of rotating machinery incremental and apparent inductances by an energy perturbation method," *IEEE Power Eng. Rev.*, vol. PER-2, no. 12, pp. 28–29, Dec. 1982.